Electronic Supplementary Material (ESI) for Materials Horizons.
This journal is © The Royal Society of Chemistry 2023

SUPPORTING INFORMATION

Polymorph Screening at Surfaces of a Benzothieno-Benzothiophene Derivative: Discovering New Solvate Forms

Ann Maria James,[a] Nemo McIntosh,[b] Félix Devaux, Patrick Brocorens,[b] Jérôme Cornil,[b] Alessandro Greco,[c]Lucia Maini,[d] Priya Pandey,[d] Lorenzo Pandolfi, [e] Birgit Kunert,[a] Elisabetta Venuti,[e] Yves Henri Geerts,[f,g] Roland Resel,[a]

[a] Institute of Solid State Physics, Graz University of Technology, Petersgasse 16, 8010 Graz, Austria

[b] Laboratory for Chemistry of Novel Materials, University of Mons, 7000 Mons, Belgium

[c] Max Planck Institute for Polymer Research, 55128 Mainz, Germany

[d] Dipartimento di Chimica “G. Ciamician”, University Bologna, 40126 Bologna, Italy

[e] Dipartimento di Chimica Industriale “Toso Montanari” ,Università di Bologna viale del Risorgimento, 4, 40136, Bologna, Italy

[f] Laboratoire de Chimie des Polymères, Université Libre de Bruxelles (ULB), 1050 Bruxelles, Belgium

[g] International Solvay Institutes of Physics and Chemistry, Université Libre de Bruxelles, 1050 Bruxelles, Belgium

In order to detail the experimental results, a number of additional experimental results are given. The corresponding importance is mentioned in the main manuscript. A short description is given below.

Figure S1 gives specular X-ray diffraction curves of films prepared by drop casting at different temperatures; specular X-ray diffraction of phase pure films of the three new phases (Form IV, V, and VI) are given at large q-values (large 2θ angles) in Figure S2, the results at low q-values (low 2θangles) are depicted in Figure 1c. Table S1 gives the preparation condition of concomitant phases, and the resulting X-ray diffraction patterns are given in Figure S3.
Figure S4 gives X-ray diffraction results on a film of Form I prepared by drop casting from chloroform solutions. Grazing incidence diffraction and in-situ temperature specular X-ray diffraction are given for comparison to the results on Form IV, V, and VI depicted in Figure 3 and Figure 4 in the main paper.
Table S2 gives the lattice constants of the new phases obtained by indexing the grazing incidence X-ray diffraction pattern and of the known phases for comparison.
Figure S5 gives the Raman spectra recorded for the three new phases. The high-frequency Raman Spectra (1000-2000 cm^{-1}) were acquired using a Renishaw inVia Raman Spectrometer. A Renishaw 785 nm laser was used as the excitation source, and the detector used was a 1024 × 256-pixel Peltier-cooled RenCam CCD detector. The time taken for the collection of one Raman spectrum was 3 minutes.
Figure S6 gives the X-ray fluorescence and Fourier transform infrared spectroscopy measured on bare silicon, for Form I, IV, V, and VI. The presence of chlorine atoms within thin films was proofed by X-ray fluorescence (XRF), a PANalytical Epsilon-1 spectrometer with an Ag source, and an energy dispersive detector was used in combination with an Al filter with a thickness of 50 µm. Fourier-transformed infrared spectroscopic (FTIR) measurements were carried out with a Bruker IF66v/ spectrometer with a liquid N_2-cooled mercury cadmium telluride (MCT) detector in the same vacuum system. Measurements in transmission mode were performed at 7 mbar for 10 min (~4000 scans) with a resolution of 4 cm^{-1}.
Figure S7 gives a specular X-ray diffraction pattern of Form IV crystals heated at 413 K for 30 minutes and subsequently recrystallized at room temperature. It is part of a large measurement series investigating the recrystallization behaviour of Form IV samples after heat treatment at various temperature ranges above their observed melting temperature.

Figure S8 gives the experimental result of the fourth phase found by using 1,2- dichlorobenzene as a solvent including specular X-ray diffraction, Grazing incidence diffraction, temperature-dependent in-situ X-ray diffraction, and Raman spectroscopy.

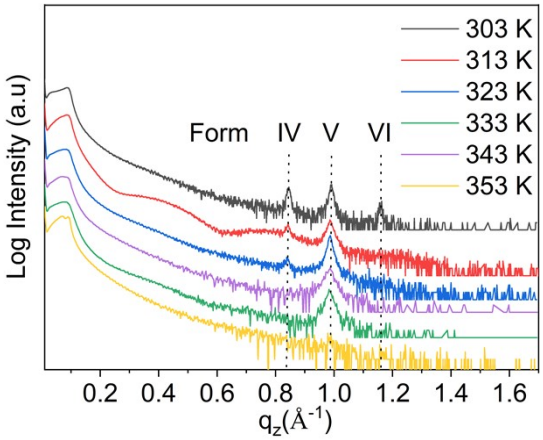

Figure S1. Specular X-ray diffraction pattern of OEG-BTBT thin films prepared by drop casting from dichloromethane solutions at different deposition temperatures.

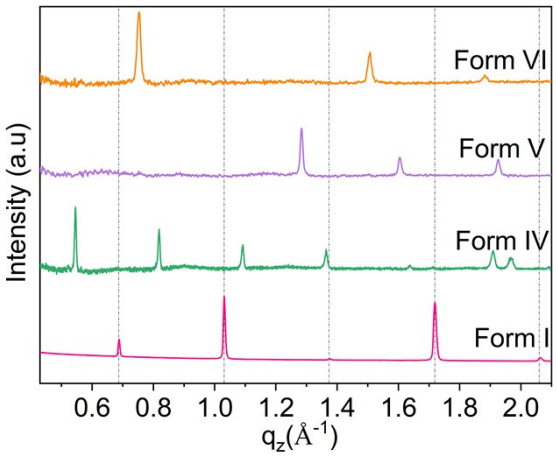

Figure S2. X-ray diffraction patterns of three thin film phases (Form IV, V, and VI) were found by drop casting of OEG BTBT molecules from dichloromethane solutions. The pattern of Form I (magenta) is shown for reference.

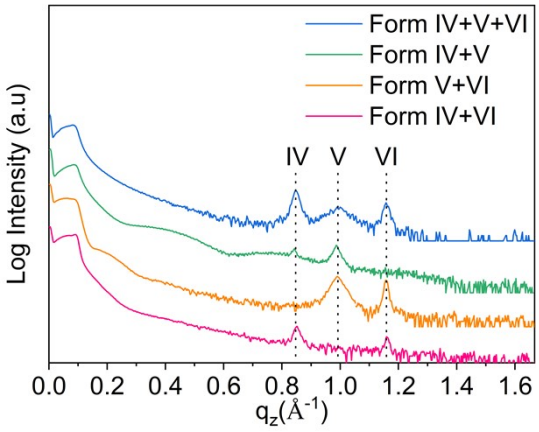

Figure S3: Specular X-ray diffraction patterns of coexisting phases of the molecule OEG-BTBT observed within thin films prepared from dichloromethane; detailed preparation conditions are listed in Table 1.

phase	thin film preparation conditions
Form IV+V+VI	from **DCM:** - drop casting at 303 K
Form IV+V	from **DCM:** - drop casting at 313 K / 323 K
Form IV+VI	from **DCM:** - drop casting from 3 g/l concentration
Form V+VI	from **DCM:** - drop casting from 3 g/l concentration at reduced evaporation rate

Table S1. Combination of coexisting phases of the molecule OEG-BTBT observed within thin films from dichloromethane, together with the respective preparation parameters.

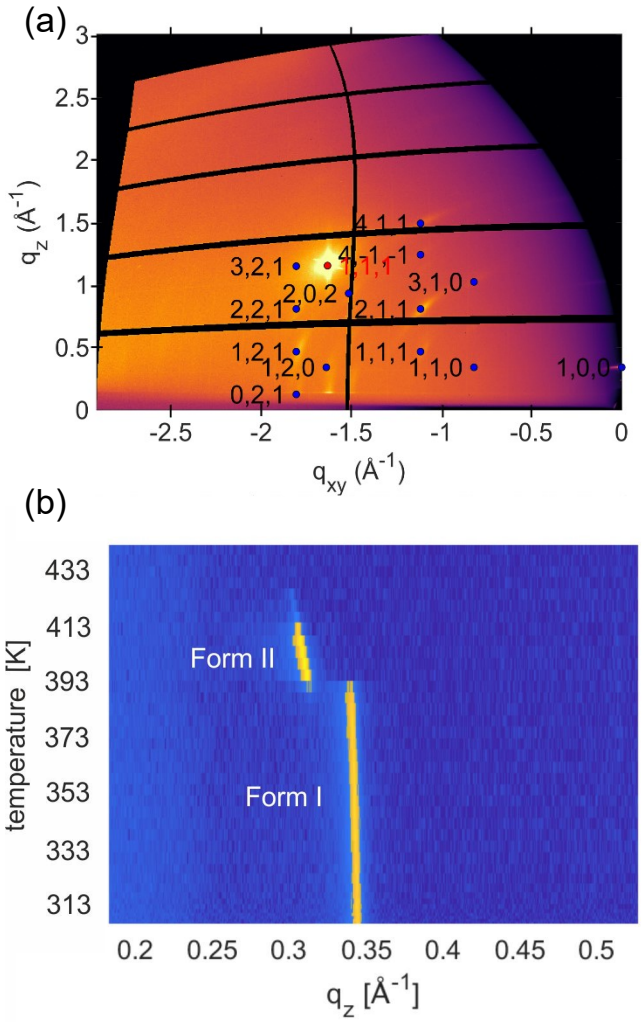

Figure S4. X-ray diffraction studies of an OEG-BTBT thin film prepared by drop casting from a chloroform solution. a) Grazing incidence x-ray diffraction; the Bragg peaks are indexed on basis of Form I with (001) preferred orientation of the crystallites (blue points) and the 111 peak of silicon (red point). b) Temperature dependent in-situ specular X-ray diffraction by decreasing temperature from the molten state back to room temperature.

	Form I	Form II	Form III	Form IV	Form V	Form VI
temperature [K]	*298*	*404*	*100*	*298*	*298*	*298*
contact plane [*hkl*]	*100*			*00-1*	*001*	*001*
a [Å]	18.63	11.653	8.3027	5.03	7.15	4.54
b [Å]	7.66	41.255	41.7587	12.13	9.34	16.28
c [Å]	8.29	8.338	7.49140	23.16	19.87	17.99
α [deg]	90	90	90	96.16	90.29	110.70
β [deg]	99.35	64.552	90	91.92	99.60	97.07
γ [deg]	90	90	90	95.30	90.08	90.12
Δq_{xy} [Å^{-1}]				0.011	0.014	0.005
Δq_z [Å^{-1}]				0.005	0.003	0.003

Table S2. Lattice constants of the three known phases (Form I, II and III) taken from the literature [41] and of the three additional phases found by drop casting from dichloromethane (Form IV, V, and VI). The temperature of the respective unit cells is given, together with the preferred orientation of the crystallites by the Miller indices of the contact plane i.e. the crystallographic plane parallel to the substrate surface. Δq_{xy} and Δq_z are the indicated errors in the two components of the scattering vector.

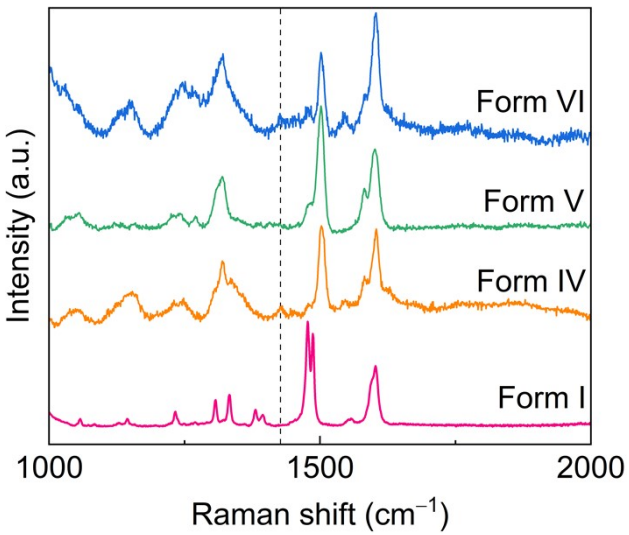

Figure S5. High-Frequency Raman Spectra recorded for three thin film phases of OEG-BTBT (Form IV, V, and VI) obtained from dichloromethane solutions. The pattern of Form I (magenta) is shown for reference. The vertical line corresponds to the characteristic Raman peak of dichloromethane at 1423 cm^{-1}.

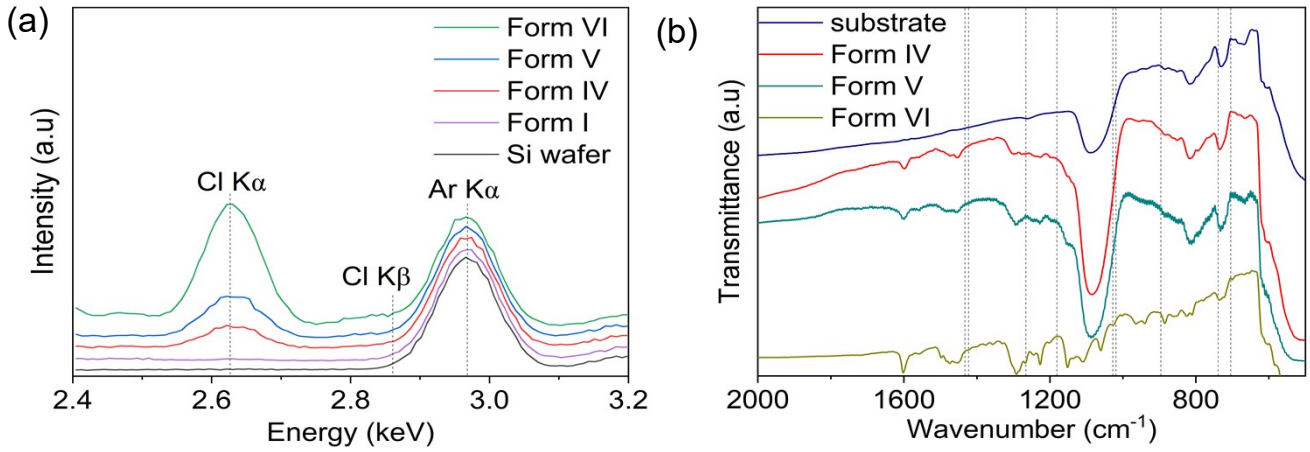

Figure S6. (a) X-ray fluorescence spectra recorded on the bare silicon substrate, drop casted films from dichloromethane (Form IV, V, and VI), and drop casted film from chloroform (Form I) (b) Fourier transform infrared spectra recorded on the bare silicon substrate and drop casted films from dichloromethane (Form IV, V, and VI). Vertical lines correspond to the characteristic peak positions (strong and weak) of dichloromethane.

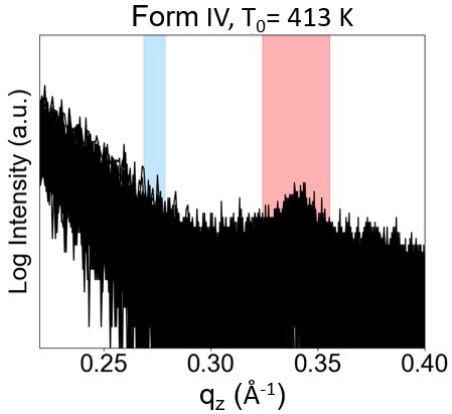

Figure S7. Recrystallization recorded for a phase pure film of Form IV which was annealed at 413 K for 30 minutes by using XRD. During recrystallization, the XRD spectra were recorded continuously while cooling down to 303 K. The characteristic peak positions of Form I (red region) and Form IV (blue region) are indicated. Here a single measurement was taken within three minutes.

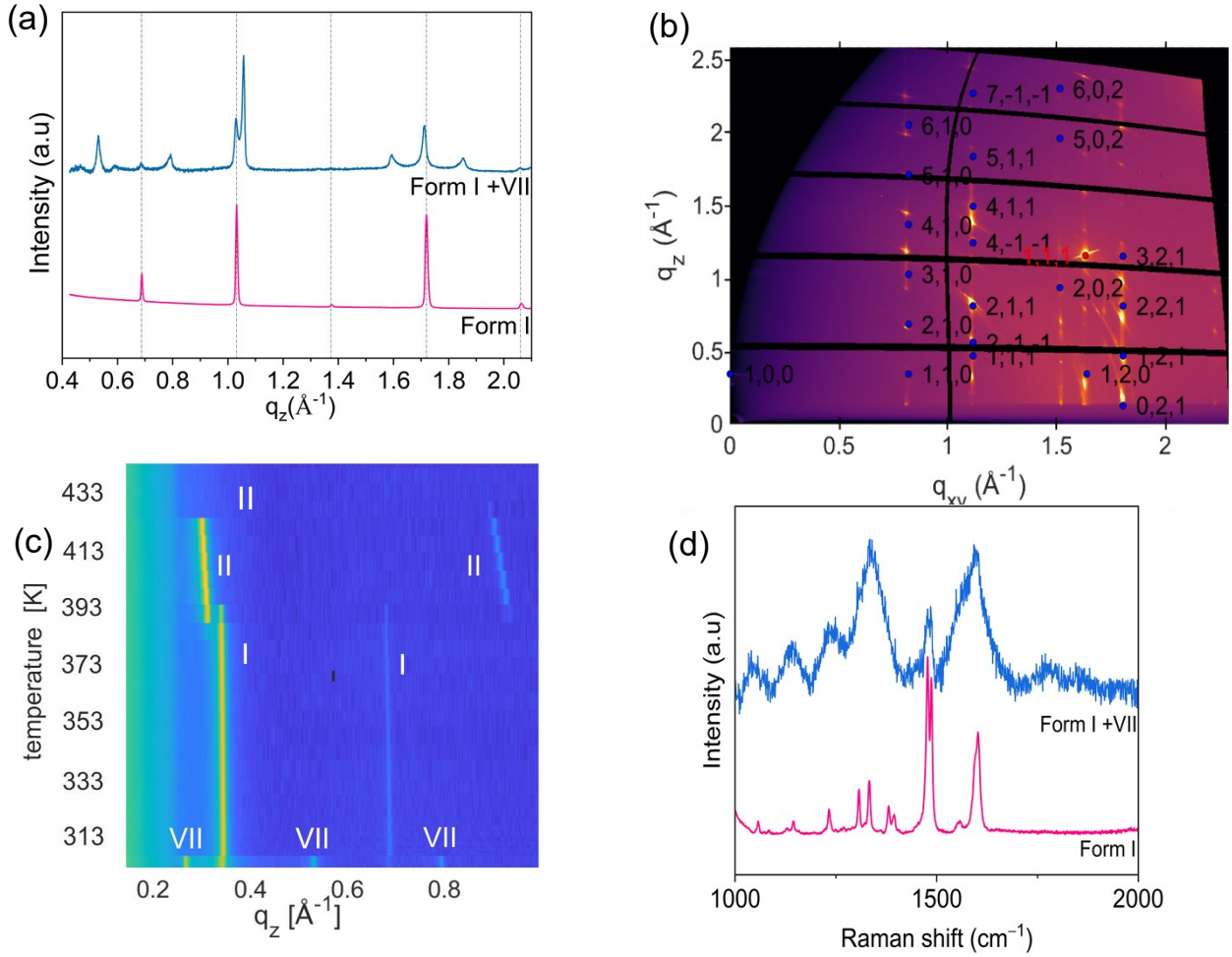

Figure S8. Experimental results of an OEG-BTBT film prepared from 1,2-dichlorobenzene revealed an unknown phase (Form VII) and the equilibrium phase Form I. a) Specular X-ray diffraction at large scattering angles 2θ, b) grazing incidence X-ray diffraction pattern with indexed Bragg peaks of Form I, c) in-situ temperature XRD with increasing temperature in a waterfall plot; the observed peaks are assigned to the different phases and d) Raman spectroscopy at large wavenumbers.